Journal of Mining and Earth Sciences
Website: https://jmes.humg.edu.vn

Assessment of a rock planar slide along an expressway in Vietnam

Nghia Tuan Do [1,*], Lan Chau Nguyen [2], Tuan Quang Nguyen [1], Dinh Quoc Nguyen [3]

[1] *Thuyloi University, Hanoi, Vietnam*
[2] *University of Transport and Communications, Hanoi, Vietnam*
[3] *Phenikaa University, Hanoi, Vietnam*

ARTICLE INFO

Article history:
Received 24th Nov. 2024
Revised 06th Mar. 2025
Accepted 21st Mar. 2025

Keywords:
Countermeasure,
Ha Coi formation,
Rock planar slide,
Slope stability.

ABSTRACT

This paper presents an assessment of a rock planar slide, which took place at km 108 along the Tien Yen-Mong Cai expressway, an extension of the Halong-Vandon expressway in Vietnam. Half of the expressway has been covered by a large volume of rock deposit after its movement. The height of the slope in this study is 16 m and its width is 200 m. The main head scarp is about 11 m high. The sliding angle of the failure surface is from 12÷15^0. The stratigraphy mostly consists of weathered jointed siltstone, which is located in the upper part of the Ha Coi formation ($J_{1\text{-}2}hc_2$). The sedimentary rocks are thick bedded, fine-grained sandstones interbedded with medium-bedded chocolate pink siltstones or thin-bedded shales. In general, they are medium to thick bedded with the thickness of rock layer from 0.3÷0.8 m. The upper rock layer is the 9b-1 layer with RQD = 0÷36% whereas the lower one is the 9b-2 layer with RQD = 0÷92%. The topsoil layer is 0.5÷2.5 m thick. Rockplane and Plaxis computer softwares were adopted to perform stability analysis of the slope. Results showed that the overall factor of safety of the slope before treatment is lower than 1.0, which is in good agreement with the instability of the slope. In order to apply the countermeasures, part of the slope will be first excavated with an angle of 45^0. Then, the prestressed ground anchor system will be installed. After treatment, the overall factor of safety of the slope was increased to larger than 1.30, which meets the requirement by the Vietnam code.

*Corresponding author
E - mail: dotuannghia@tlu.edu.vn
DOI: 10.46326/JMES.2025.66(2).05

1. Introduction

So far, landslides have taken place in many countries throughout the world and become one of the most prominent geo-hazards. In particular, construction activity often changes the initial limit equilibrium state of slopes along expressways and hence trigger landslides in the vicinity of such roads. Besides, many researchers have considered heavy and/or long rainfall events as one of the main causative factors. Rainfall events can not only erode topsoils but also raise the groundwater table in the slope, leading to a decrease in the shear strength of subsoils (Bayer et al., 2018; Gong et al., 2021). Many researches have been performed on slope stability (Dang et al., 2019; Nguyen et al., 2020). However, most of them focus on the soil slide instead of the rock planar slide. Besides, in order to calculate the factor of safety of slope, the limit equilibrium method and finite element method with reduced shear strength are widely used. These methods can be performed by many computer softwares, such as Plaxis, Rockplane, Flac, Geo studio, etc. For rock planar sliding, it seems that Plaxis and Rockplane softwares are easier to use and model accurate the slope conditions (Mokhtar and Rad, 2020; Oberhollenzer et al., 2018, Zheng et al., 2009, etc.).

In this study, a rock planar slide happened at km 108 along the Tien Yen-Mong Cai expressway, which is an extension of the Halong-Vandon expressway in Vietnam will be investigated. Besides, the Plaxis and Rockplane softwares will be adopted to estimate the effectiveness of countermeasures proposed for this slope.

2. Study Area

2.1. Overview Of The Landslide

The location of the slope is Tan Binh Commune, Dam Ha district, Quang Ninh Province, which is in the northeast part of Vietnam. The rock slope is located at the section from km108 + 150 to km108 + 350 on the left cut slope (Figure 1) with the coordination of $21^{0}24'40''$ N and $107^{0}37'55''$ E. The sliding occurred after the excavation of the slope. In order to determine causes and put forward countermeasures, field surveys and soil investigation have been performed to investigate the distribution of cracks and retrieve soil and rock samples. Figure 2 is the topographic map of the study area. Although the debris material has been cleared, the remaining slope still can threaten the expressway in the long term if its stability is not guaranteed.

The sliding area is 7000 m^2, 200 m wide, about 70 m long, and 16 m high. The volume of sliding rock is estimated at 70000 m^3 with a sliding direction of 150^0. The sliding area locates at the siltstone and shale of the Ha Coi formation. The stratigraphy mainly consists of highly to moderately weathered and interbedded siltstone and shale. The sliding surface has occurred in moderately weathered shale, which has low mechanical properties, as shown in the left top corner in Figure 1. It seems that the weak bedding plane has played an important role in causing the rock slide in addition to other unfavourable factors such as rainfall and human activity, etc.

2.2. Geological Setting

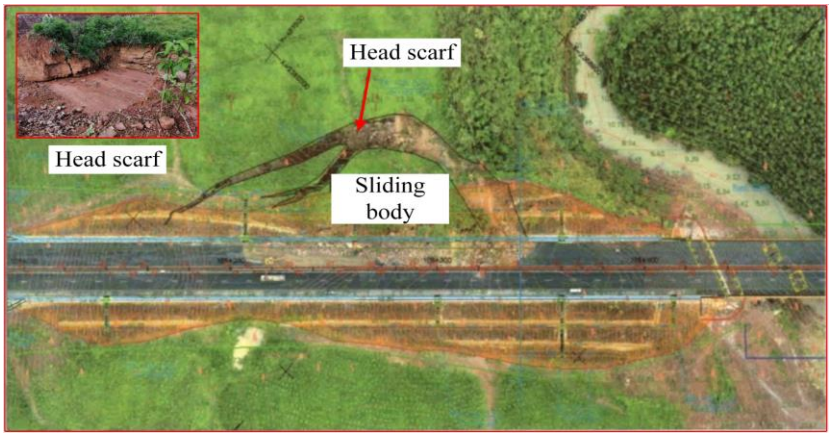

Figure 1. Overview of the rock slide.

2.2.1. Topographical condition

The rock slope is located at the hilly terrain. With respect to topographical condition, the slope surface is originally convex with the elevation of 31.0÷72.0 m. The original hill slope is southeast facing whereas the expressway's direction is from southwest to northeast. The slide direction is nearly the same as the slope aspect outward. The height of the cut slope is 16 m. As shown in Figure 2, the arc-shaped sliding has moved from the original slope toward the expressway and the maximum distance of detachment is 25 m. The main head scarp is about 11 m high. The sliding angle of the failure surface is from 12÷15^0, which matches that of the bedding plane.

2.2.2. Lithology and geological structure

Based on the Vietnam geological map (Figure 3), the rock slide is located in the upper part of the Ha Coi formation ($J_{1\text{-}2}hc_2$), which is Jurassic red continental sedimentary rocks. Also, they are thick bedded, fine-grained sandstones interbedded with medium-bedded chocolate pink siltstones or thin-bedded shales. In general, the sedimentary rocks are medium to thick bedded with the thickness of rock layer from 0.3÷0.8 m. At some locations, their thickness is even greater, as shown in Figure 4. Tectonic movements have taken place in the area of the rocks and made them folded and slightly foliated. The rock bedding dip is the southeast and the dip direction is from 140÷180^0 whereas the dip angle is from 10÷12^0. The rocks are moderately jointed in general, at which the bedding planes and fractures are random and not consistent.

Bedding joints are the major structural features of the rock layer in the site with a dominant orientation (Figure 4). As shown in Figure 5, a thin film of calcite infill could be observed at most of bedding joints, which is attributed to the existence of groundwater in joints causing calcite to precipitate. This infill material with low shear strength will contribute to the sliding of the rock slope. In addition, strong rock layers, including siltstone, fine quartz sandstone, are sandwiched by highly weathered shale layers, which are easily softened under saturated conditions. These thin shale layers could become potential sliding surfaces of the

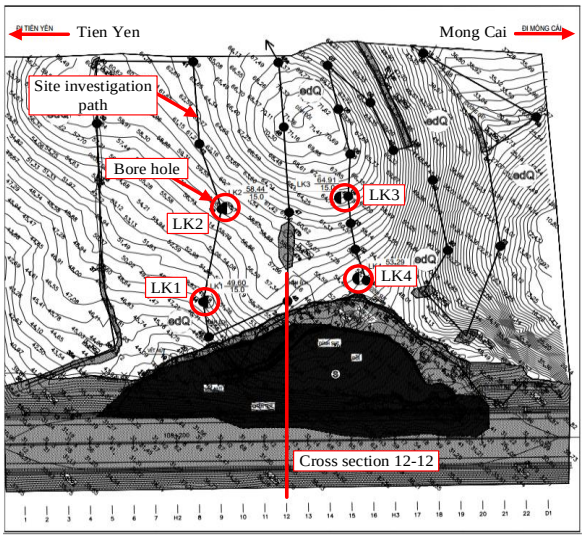

Figure 2. Topographic map and borehole layout of the rock sliding area Do et al. (2024).

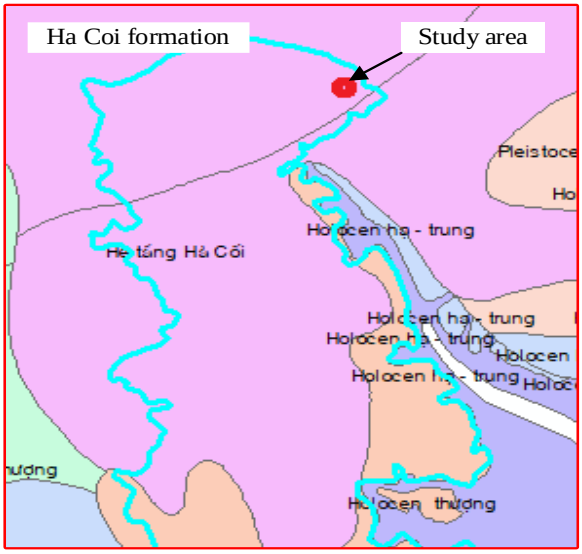

Figure 3. Geological map of the study area.

Figure 4. Interbedded siltstone at the head scarp of slope failure Do et al. (2024).

slope (Figure 5). Based on the rock mass quality, two bedrock layers can be characterized, including moderately weathered horizon and slightly weathered horizon ones. There is a residual and colluvium soil layer, which overlays the bedrock. Section 2.3 will describe the characteristics of soil and rock layers in detail.

2.2.3. Kinematic analysis of slope

The rock slide can be classified as a planar sliding type due to its characteristics as shown in Figs. 1, 2, 4, and 5. The study by Hoek and Bray (1981) has addressed the kinematic conditions for a plane mode of failure when the strike difference between the slope face and the potential failure surface is almost parallel ($\pm 20^0$). Also, the lateral surfaces on both sides of the sliding block would not provide any resistance against the sliding. A plane failure may occur when a discontinuity dips in a similar direction to the slope surface, which is smaller than the slope angle but greater than the friction angle along the failure plane. There is no side effect to the stability of the slope because the slope surface is convex. The stereographic projection slope section with the dominant bedding planes and the cut slope face is shown in Figure 6. Potential plane failure can be observed in this figure. If it is assumed that the shear strength of the bedding joint is contributed from the friction angle only, the planar failure will take place once the friction angle is lower than the dip angle of bedding planes, i.e., from $12 \div 15^0$

2.3. Soil And Rock Properties

Four bore holes have been performed in the site as marked by LK1, LK2, LK3, and LK4 in Figure 7 to determine soil stratigraphy and characteristics of soil and rock layers. It is observed that the stratigraphy consists of three soil and rock layers. The soil layer 8 is located at the top of the slope surface, which is very stiff to hard sandy clay with grits and boulders. This layer is from 0.5÷2.5 m thick. Beneath this layer is the moderately weathered layer (layer 9b-1), which is violetish brown, highly jointed, hard to medium hard siltstone, and shale with poor quality indexes TCR = 25÷83% and RQD = 0÷36%. This layer is from 0.5÷3.0 m thick. The slightly weathered, medium-jointed siltstone (layer 9b-2) is located at the bottom of the stratigraphy. This layer has rather good quality indexes with TCR = 60÷97% and RQD = 25÷92%. The thickness of this layer is greater than the borehole depth. In general, this layer can be characterized as good to very good rock. It is noted that this is an inhomogeneous layer inserted with the thin layers of soft rock or highly fractured rock corresponding to fair to poor rock.

Tables 1 and 2 summarize the results of laboratory tests for the soil and rock layers, respectively. In order to perform stability analysis, the cohesion and friction angles at both natural and saturated states were determined for the soil layer 8.

Figure 5. Smooth sliding surface of the rock layer.

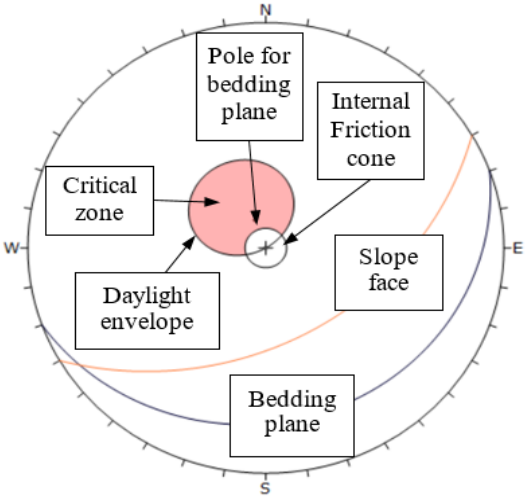

Figure 6. Kinematic analysis of the slope stability Do et al. (2024).

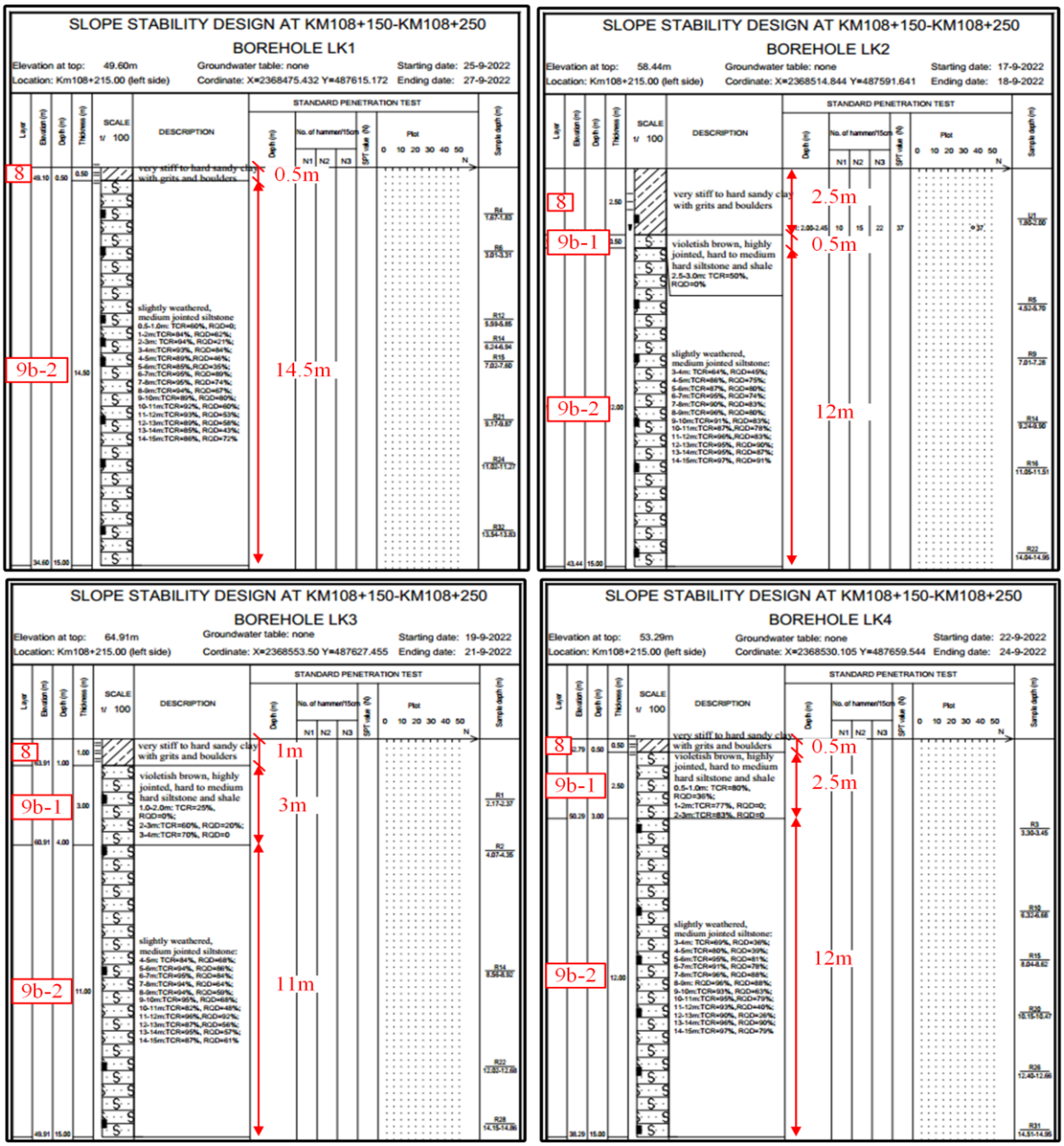

Figure 7. Soil profiles at different boreholes.

Table 1. Soil properties from laboratory tests.

Properties	Layer 8	Properties	Layer 8
Type of soil (USCS)	CL	Degree of saturation, S_r (%)	91.22
Water content, w (%)	22.1	Liquid limit, LL (%)	38.0
Natural unit weight, γ (kN/m^3)	20.0	Plastic limit, PL (%)	22.0
Dry unit weight, γ_d (kN/m^3)	16.4	Plasticity index (%), PI	16.0
Saturated unit weight, γ_{sat} (kN/m^3)	20.4	Coefficient of compressibility, $a_{v,1-2}$ (1/kPa)	0.017
Specific gravity, G_s	2.72	Effective cohesion at natural state, c (kPa)	25.5
Porosity, n (%)	39.72	Effective internal friction angle at natural state, ϕ (^{0})	23^{0}05’
Void ratio, e	0.659	Effective cohesion at saturated state, c (kPa)	17.7
		Effective internal friction angle at saturated state, ϕ (^{0})	18^{0}58’

Uniaxial compressive strength at natural and saturated states was estimated for the rock layers (layers 9b-1 and 9b-2). The other properties of soil and rock layers can be seen in these tables.

Figure 8 is the representative cross-section of the study slope (cross-section 12-12). This cross-section is located at the center of the sliding body, which passes through the headscarf (as marked in Figure 2). The stratigraphy after the site investigation is also presented in the figure, at which the soil and rock layers have been shaded. Besides, the sliding body after measurement is plotted in the figure to determine the failure surface.

3. Slope Stability Analysis

In order to perform a stability analysis of the slope, the Rockplane and the Plaxis computer softwares were adopted. The Rockplane software estimates the overall factor of safety of the slope based on the limit equilibrium method. On the other hand, the Plaxis software makes use of the finite element method coupled with the strength reduction technique. This software can simulate all of the soil conditions and characteristics of retaining system in analysis. Also, the failure surface of soil/rock can be predicted in the software only based on the distribution of plastic points without any pre-assumptions.

3.1. Input parameters of soil and rock layers

The input parameters of soil and rock layers are summarized in Table 3. For simplicity, it was assumed that the behaviors of all the soil and rock layers were elastic perfectly plastic, which could be simulated using the Mohr-Coulomb model.

Table 2. Rock properties.

Parameters	Layer 9b-1	Layer 9b-2	Parameters	Layer 9b-1	Layer 9b-2
Unit weight, γ (kN/m^3)	25.5	26.5	s	9.22×10^{-6}	3.93×10^{-5}
Intact compr. strength, σ_i (MPa)	17.1	37.1	a	0.544	0.522
Geological Strength Index (GSI)	20	30	Cohesion, c_m (MPa)	0.049	0.105
Intact Rock Constant, m_i	7	7	Friction, φ_m (degree)	21.79	32.79
Disturbance Factor, D	0.7	0.7	Young modulus, E_m(MPa)	4.779	1251.8
m_b	0.086	0.15	Poisson's ratio, ν	0.2	0.2

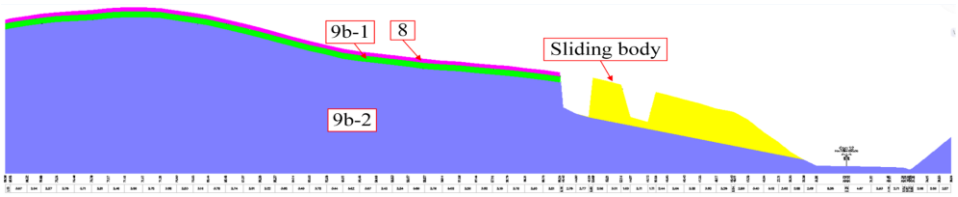

Figure 8. Cross section 12-12.

Table 3. Input parameters for Plaxis 2D model.

Parameter	Symbol	Unit	Layer 8	Infill material	Layer 9b-1	Layer 9b-2
Type of model			Mohr-Coulomb			
			Undrained		Drained	
Unsaturated unit weight	γ_{unsat}	kN/m^3	19.0	19.0	25.0	25.0
Saturated unit weight	γ_{sat}	kN/m^3	20.4	20.4	26.0	26.5
Effective cohesion at natural state	c'	kPa	25.5	20	49	116
Effective internal frictional angle at natural state	ϕ'	^{0}	23.1	13.4	21.8	34.4
Effective cohesion at saturated state	c'	kPa	17.7	15.0	36	105
Effective internal frictional angle at saturated state	ϕ'	^{0}	18.9	10.1	17.8	32.6
Poisson's ratio	ν	-	0.3	0.3	0.2	0.2
Elastic modulus at natural state	E_{ref}	kN/m^2	2.2E+4	2.2E+4	4.8E+5	1.4E+6
Elastic modulus at saturated state	E_{ref}	kN/m^2	1.7E+4	1.7E+4	3.6E+5	1.1E+6

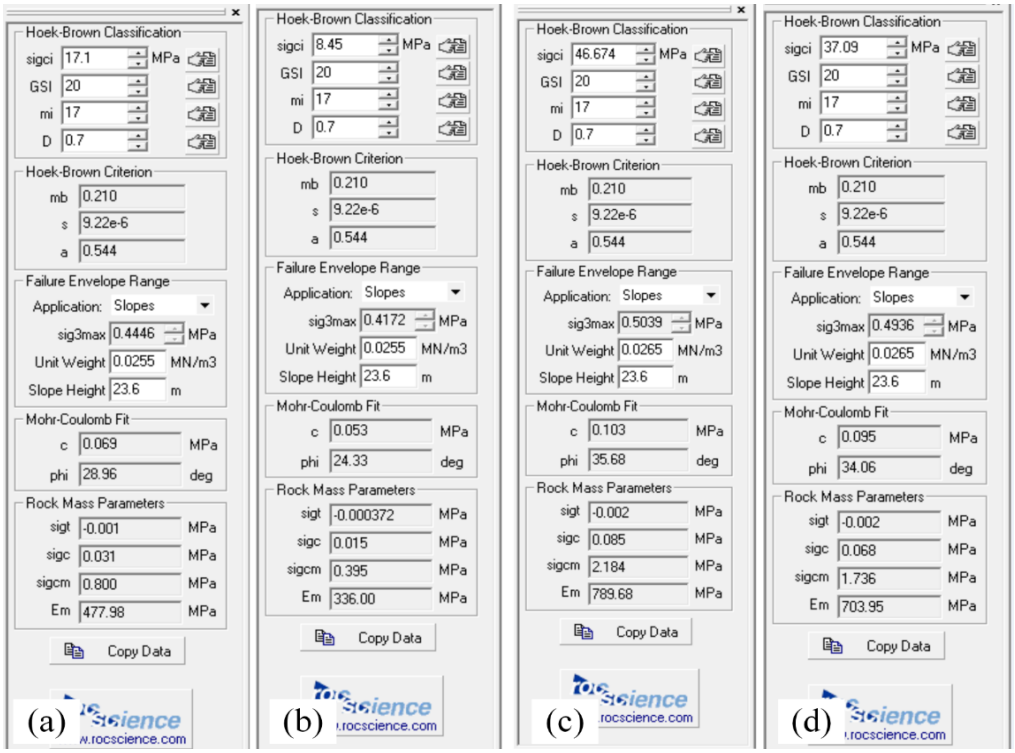

Figure 9. Input parameters of soil and rock layers estimated by Rocklab: (a) 9b-1 rock layer at natural state; (b) 9b-1 rock layer at saturated state; (c) 9b-2 rock layer at natural state; (d) 9b-2 rock layer at saturated state.

This model requires five input parameters, including Young's modulus (E), Poisson's ratio (ν), friction angle (ϕ), cohesion (c), and dilatancy angle (ψ). The soil layer 8 and infill layer were simulated using undrained behavior due to the high content of clay particles and the rock layers were modelled using drained behavior because of their strongly weathered cracks. Particularly, for the soil layer 8, the shear strength parameters were taken from laboratory tests. For the rock layers 9b-1 and 9b-2, these parameters were estimated using the Roclab program based on the characteristics of rock (Figure 9).

The effective natural friction angle of the infill material was estimated at 13.4^0, which was equal to the average inclined angle of the bedding planes of rock. Based on the manual for river works in Japan by the river bureau, ministry of construction (1997), the effective natural cohesion of the infill material was assumed at 20 kPa according to the slope height of 15÷20 m. For the rock layers and the infill material, the shear strength at the saturated state was taken at 75% of those at the natural state.

3.2. Numerical model

Figure 10 is the input parameters adopted in Rockplane at which the failure plane angle is 13.4^0 based on the observation in the site. The sliding surface of the rock slope is shown in Figure 11 along the failure plane. The acting forces on the sliding body can be referred to in Figure 12.

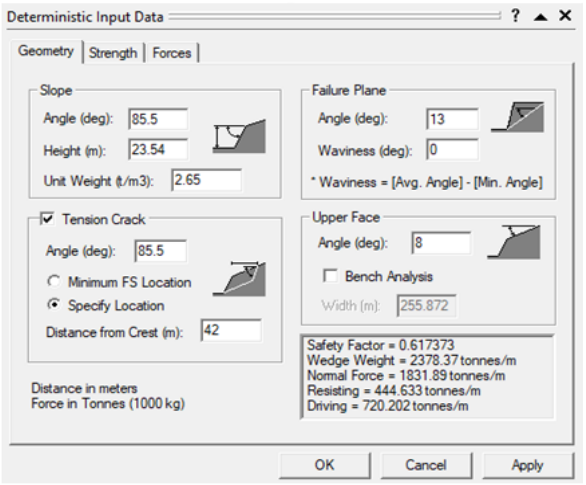

Figure 10. Input data and results in Rockplane at cross section 12-12.

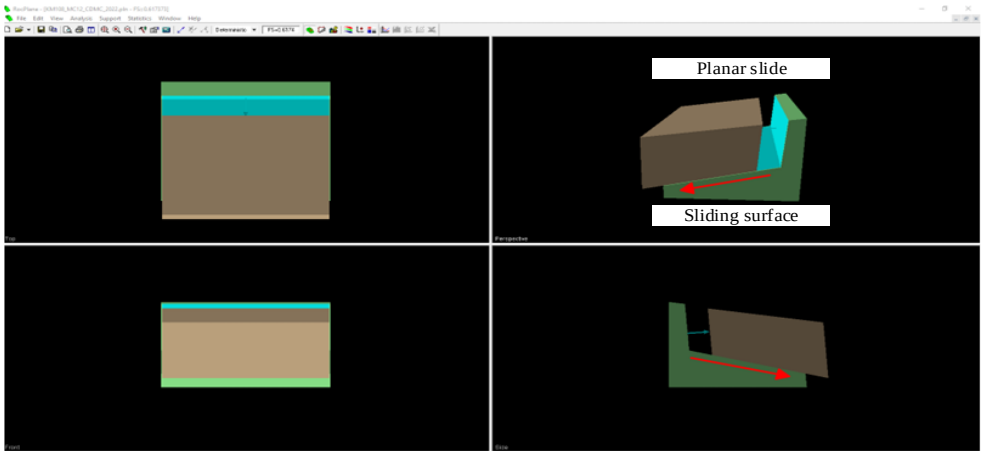

Figure 11. Planar slide in Rockplane at cross section 12-12.

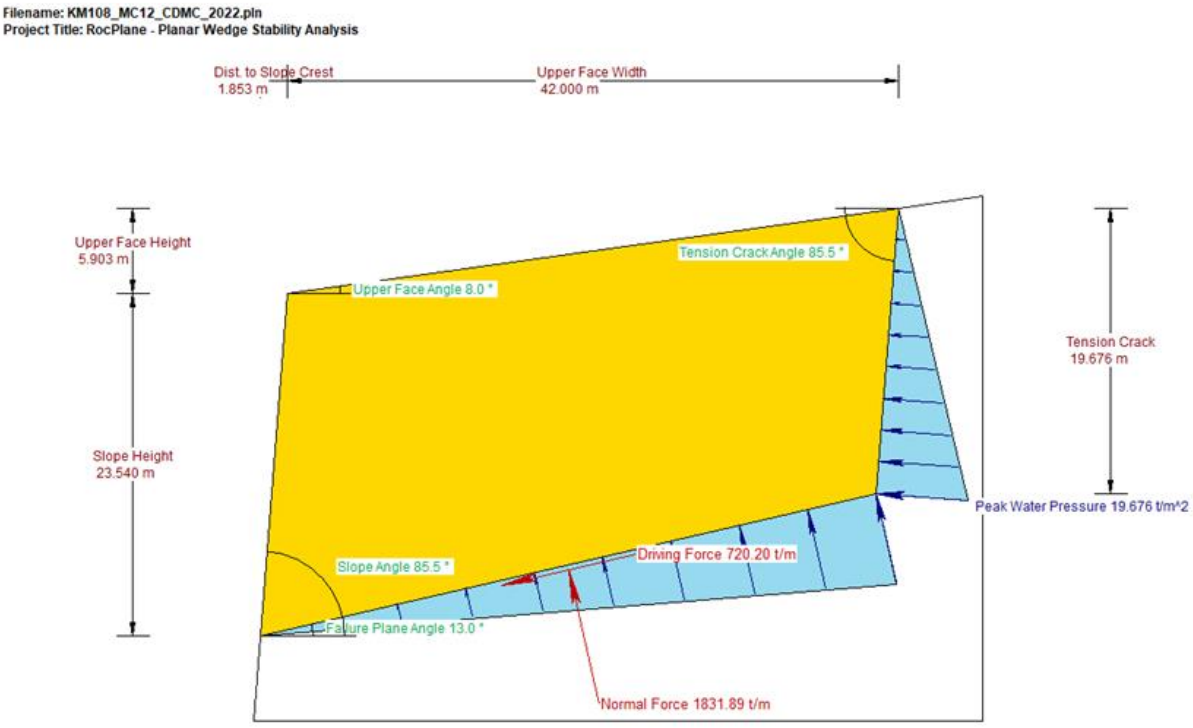

Figure 12. Acting forces on the sliding body in Rockplane at cross section 12-12.

Figure 13a is the numerical model of the slope in Plaxis. As shown in Figure 13b, the infill material was simulated using thin strips, which inclined 13.4^0 with respect to the horizontal line. It was assumed that these strips ranged throughout the slope. Figures 13c and 14 are total incremental displacement plots of the slope in stability analysis before and after treatment, respectively. It is noted that the location of the groundwater table before treatment was assumed near the ground surface based on the state of soil and rock layers in the site observed by the authors during the investigation. On the other hand, after treatment, since the horizontal pipes (L = 10 m) have been designed to reduce the groundwater table if any in the slope, the location of the groundwater table was assumed close to the depth of the horizontal pipes as an unfavorable case.

4. Results and Discussions

As shown in Figure 10, the overall factor of safety estimated by Rockplane is 0.62, which is

much lower than 1.0, indicating the instability of the slope.

As using the Plaxis software, the total incremental displacement plot of the slope at the initial state in stability analysis is shown in Figure 13c. Since the total incremental displacement represents the velocity of soil/rock movement at the last calculated step, this displacement will be very large if the slope approaches an unstable state. Based on the development of the total incremental displacement, the sliding surface of the slope could be determined in the figure, which matches well with the distribution of cracks measured in the site. The overall factor of safety estimated by the Plaxis software was 0.69. This result is very close to that of Rockplane and also indicates an unstable state of the slope. It should be noted that in principle, Plaxis uses the strength reduction method (SRM) to calculate the factor of safety, at which the shear strength parameters of soil and rock layers are progressively reduced until the slope fails. The ratio of the original strength to the reduced strength at failure is defined as the factor of safety (FS) of the slope. The Rockplane, on the other hand, relies on the limit equilibrium method to define the FS value as the ratio between the resistance force to the driving force. Thus, the FS values, which are lower than 1, just merely indicate how seriously the slope is unstable. Many researchers have adopted this method and put forward the FS values lower

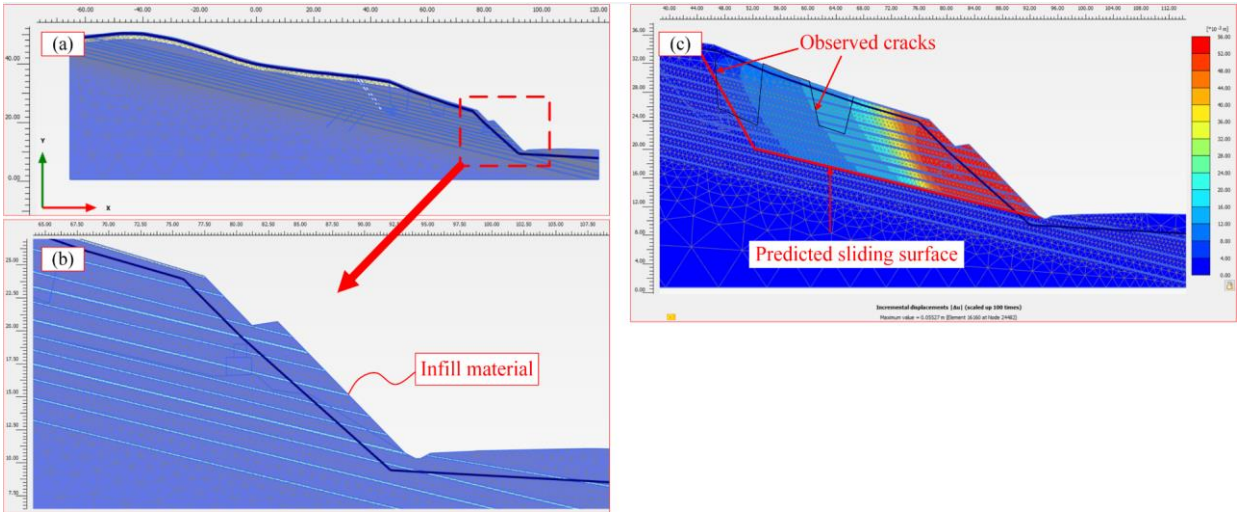

Figure 13. Numerical model of cross section 12-12 for the initial rock slope in Plaxis.

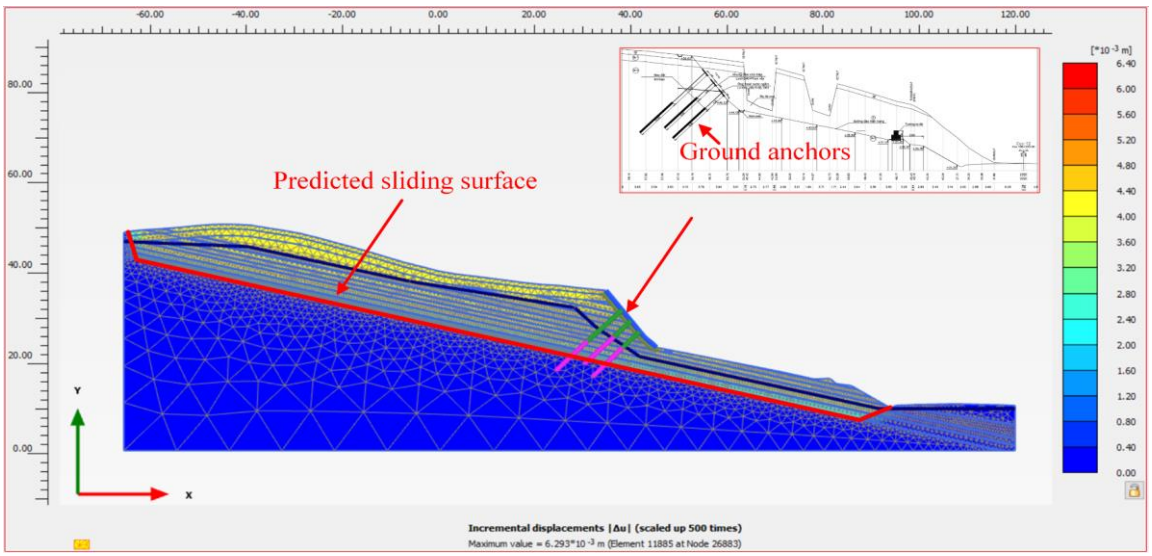

Figure 14. Total incremental displacement plot in stability analysis of the retained rock slope in Plaxis.

than 1.0 such as Amarasinghe et al. (2024), Deng et al. (2017), Hammah et al. (2005), etc.

In order to retain the slope, the sliding soil and rock layers were first removed. The slope angle was created at 45^0. Horizontal drainage pipes with 10 m length were applied to reduce the groundwater table. Three layers of prestressed ground anchors with lengths of 15 m and 20 m were installed. The anchor spacing was 4 m and each of the anchors was applied a preload of 250 kN. Besides, a gabion wall was constructed along the slope toe to prevent rocks from falling into the expressway. The predicted sliding surface of the slope after treatment is shown in Figure 14, at which the ground anchors are still located beyond this surface. The overall factor of safety estimated by Plaxis is 1.381. This result is greater than the required value of 1.3 by the Vietnam code for the expressway (2021). Therefore, the designed countermeasures meet all of the requirements.

5. Conclusions

Some following conclusions can be drawn based on the results of this study on the stability of the slope at km 108 along the Tienyen - Mongcai expressway in Vietnam, which is an extension of the Halong-Vandon expressway in Vietnam:

i. Since the main planar sliding surface occurred along the bedding joints of the rock layers, the failure of the slope could be classified as the rock planar slide.

ii. The overall factors of safety predicted by Rockplane and Plaxis softwares were 0.62 and 0.69, respectively for the slope at the initial state, which are in good agreement with the unstable state of the slope in the site. Hence, these softwares can estimate well stability of the slope.

iii. After treatment, the overall factor of safety of the slope was 1.381 > 1.3 by the Vietnam code for the expressway (2021) and the ground anchor was still located beyond the predicted failure surface. Therefore, the countermeasures meet all of the requirements.

Acknowledgments

This research is funded by Vietnam National Foundation for Science and Technology Development (NAFOSTED) under grant number 105.08-2020.25.

Contributions of authors

Nghia Tuan Do, Tuan Quang Nguyen- methodology, writing, review & editing; Lan Chau Nguyen- review & editing; Dinh Quoc Nguyen- review & supervision.

References

Amarasinghe, M. P., Robert, D., Kulathilaka, S. A. S., Zhou, A., Jayathissa, H. A. G., (2024). Slope stability analysis of unsaturated colluvial slopes based on case studies of rainfall-induced landslides. *Bulletin of Engineering Geology and the Environment,* 83, 476.

Bayer, B., Simoni, A., Mulas, M., Corsini, A., & Schmidt, D. (2018). Deformation responses of slow-moving landslides to seasonal rainfall in the northern Apennines, measured by InSAR. *Geomorphology,* 308, 293-306.

Deng, D. P., Li, L., Zhao, L. H., (2017). Limit equilibrium method (LEM) of slope stability and calculation of comprehensive factor of safety with double strength-reduction technique. *Journal of Mountain Science,* 14, 2311-2324.

Dang, K., Sassa, K., Konagai, K., Karunawardena, A., Bandara, R. M. S., & Hirota, K. (2019). Recent rainfall-induced rapid and long-traveling landslide on 17 May 2016 in Aranayaka, Kagelle District, Sri Lanka. *Landslides,* 16(1), 155-164.

Do, T. N., Nguyen, L. C., Tuan, N. Q., & Vu, T. T. H. (2024). Rock planar slide - A case study at Tien Yen-Mong Cai expressway, Vietnam. *Proceedings of the 5th International Conference on Geotechnics for Sustainable Infrastructure Development,* 1637-1650.

Gong, S., Juang, C., & Wasowski, J. (2021). Geohazards and human settlements: Lessons learned from multiple relocation events in Badong, China - Engineering geologist's perspective. *Engineering Geology,* 285, 106051.

Hammah, R. E., Yacoub, T. E. and Corkum, B. C. Curran, J. H. (2005). The shear strength reduction method for the generalized Hoek-Brown criterion. *Proceedings of the 40th U.S. Symposium on Rock Mechanics*.

Hoek, E., Bray, J. W. (1981). *Rock slope engineering*. E & FN Spon and imprint of Chapman & Hall. London, UK, 357 pages.

Mokhtar, S., Rad, M. Y., (2020). Uncertainty Analysis of the Stability Parameters of Rock Walls. *Archives of Civil Engineering,* 16(4), 703-721.

Nguyen, L. C., Tien, P. V., & Do, T. N. (2020). Deep-seated rainfall-induced landslides on a new expressway: a case study in Vietnam. *Landslides,* 17, 395-407.

Oberhollenzer, S., Tschuchnigg, F., Schweiger, H.F., (2018). Finite element analyses of slope stability problems using non-associated plasticity. *Journal of Rock Mechanics and Geotechnical Engineering.,* 10(6), 1091-1101.

River bureau (1997). *Manual for river works in Japan*. Ministry of construction.

TCVN 13346:2021. The landslide prevention engineering on road requirements for investigation and design.

Zheng, Y., Tang, X., Zhao, S., Deng, C., Lei, W., (2009). Strength reduction and step-loading finite element approaches in geotechnical engineering. *Journal of Rock Mechanics and Geotechnical Engineering.,* 1(1), 21-30.